Adsorption 3, 165–171 (1997)

Adsorption Characteristics of Synthesized Mordenite Membranes

SATOSHI YAMAZAKI* AND KAZUO TSUTSUMI†
Department of Materials Science, Toyohashi University of Technology, Tempaku-cho, Toyohashi 441, Japan
tsutsumi@tutms.tut.ac.jp

Received January 19, 1996; Revised August 21, 1996; Accepted September 22, 1996

Abstract. Nitrogen adsorption at 77 K was measured for a self-supporting mordenite membrane synthesized on, and detached from, a polytetrafluoroethylene (PTFE) substrate, and for a simultaneously formed powder. The adsorption by the membrane saturated at an amount which was about half that found for adsorption by the powder. To examine this difference in adsorption characteristics, both of powder and membrane were measured for adsorption for water, methanol, *n*-hexane and *tert*-butyl alcohol. For methanol, *n*-hexane and *tert*-butyl alcohol, the powder and membrane both showed the same adsorption behavior as for nitrogen. When water molecules were adsorbed, however, there was no difference in saturated adsorption amount between powder and membrane, suggesting the presence of "deformed pores" in the rectangular crystal layer of the mordenite membrane. The deformed pores are assumed to occur as gaps among crystallites which displaced along the *ab* planes of the rectangular crystals, forming the rectangular crystal layer. The channel bonding sites resulting from such displacement were found to serve as pore walls against adsorbable molecules which have a cross-sectional area greater than that of the water molecule, and so to hinder their entrance into the deformed pores. X-ray diffraction analysis revealed that the rectangular crystals have no periodic, continuous structure along the *c*-axis; they show a slight distortion of the crystallite shift from the plane perpendicular to the *c*-axis.

Keywords: mordenite membrane, deformed pore structure, adsorption properties, membrane synthesis

Introduction

Mordenite is a kind of naturally-occurring zeolite of high Si/Al ratio. Since the first synthesis by Barrer (1948), a large number of mordenite syntheses have been reported. In a study aiming at increased Si/Al ratios, mordenite having Si/Al ratios of 5–10 was dealuminated to obtain Si/Al ratios of up to 600 (Kranich, 1971). Ueda et al. (1980) succeeded in direct synthesis of high-silica mordenite using an organic template. Zeolite is known to show higher heat resistance, acid resistance and solid acid strength as its Si/Al ratio increases. Since mordenite has relatively high Si/Al ratios for an ordinary synthetic compound, and is easily dealuminatable, it is as useful as a high-silica ZSM-5 zeolite.

In recent years, zeolite membranes have drawn attention, resulting in some reports (Hennepe et al., 1987; Tsikoyiannis and Haag, 1992; Sano et al., 1992; Boom et al., 1994; Sano et al., 1994) have included synthesis and applications to separation membranes. Although the "leak-free" zeolite membrane is still difficult to be prepared, the synthesized membranes are found to be efficient in separation process. We have so far synthesized the zeolite A membrane (Yamazaki and Tsutsumi, 1995) and the mordenite membrane (Yamazaki and Tsutsumi, 1995). The mordenite membrane synthesized on PTFE substrate was easily detachable from the substrate, resulting in a self-supporting membrane. This was subjected to nitrogen adsorption measurement; the surface area and saturated adsorption amount were found to be about half those of the powder.

*Present address: Department of Materials Science, Sizuoka Institute of Science and Technology, Toyosawa, Fukuroi 437, Japan.
†Corresponding author.

Although no zeolite membranes are now in common use, the expected application should stem from their adsorption characteristics. In the present study, adsorption measurements were carried out for water, methanol, *n*-hexane and *tert*-butyl alcohol, which have different molecular cross-sectional areas and polarities, to examine the adsorption behavior of the synthetic mordenite membrane. We also examined the pore structure of the membrane, on the basis of comparisons with the powder's adsorption behavior and structural analysis results.

Experimental

The samples for adsorption measurement were synthesized as follows: colloidal silica (Nissan Chemical, 40% SiO_2 contained), sodium aluminate (Kanto Chemical) and sodium hydroxide (Kishida Chemical) were used as starting sources. After each starting source was weighed out, the sodium aluminate and sodium hydroxide were dissolved in water. This aqueous solution was added to the colloidal silica to yield a hydrogel. The initial hydrogel had a composition of 3.0 Na_2O-1.0 Al_2O_3-20 SiO_2-200 H_2O as the molar ratio. The hydrogel was poured into a 30 ml PTFE vessel; a 28 × 15 × 1 mm PTFE plate was immersed in the hydrogel in an upright position. After sealing, the vessel was fixed in a water-filled 500 ml autoclave and the contents were subjected to crystallization at 453 K for 5 days. After crystallization, the resulting powder and membrane were separated, washed with water, and dried at 383 K overnight. The structures of the dried powder and membrane were determined by X-ray diffraction analysis. Also, the respective crystal forms were observed by scanning electron microscopy (SEM); the Si/Al ratios of the respective crystals were determined by attached EPMA by means of face-analysis. The calibration of EPMA was carried out by use of A-type zeolite, faujasite, mordenite and ZSM-5 with wide range of Si/Al ratios.

After saturated water adsorption, the synthesized powder and membrane were heated at 1273 K for at least 12 hours to determine loss on ignition. About 200 mg each of the powder and the membrane was weighed out and subjected to N_2 adsorption measurement at 77 K, using a volumetric adsorption apparatus. Also, adsorptions of water, methanol, *n*-hexane and *tert*-butyl alcohol were measured at 303 K by a gravimetric method using an electromicrobalance of type Cahn 2000. Prior to adsorption measurements, each sample was dried at 773 K in a vacuum of 1 mPa for 5 hours.

Results and Discussion

Figure 1 shows the X-ray diffraction patterns of the synthesized powder and membrane. Since the membrane which formed on the PTFE substrate was easily detached from the substrate, both sides of the membrane were characterized. The face in contact with the hydrogel is hereinafter referred to as the hydrogel side, and the face in contact with the PTFE substrate as the plate side. The peaks indicated by closed dots in Fig. 1 are those of the clay used to fix the membrane during measurement. The synthesized mordenite powder showed the same diffraction pattern as that shown in the literature (von Ballmoos and Higgins, 1990), demonstrating the formation of pure mordenite crystals. Under the fact that the diffraction analysis of the membranes was performed by using an X-ray source of 0.01 degree in its incident angle and a detector with a broader slit, it can be considered that peak intensity ratio of the hydrogel side of the membrane was the same as that of the powder. Thus it seems likely that the hydrogel side has the same crystalline structure as the powder. In the plate side diffraction pattern, the (200) and (202) diffraction peak intensities decreased, while the (020) diffraction intensity increased. These findings suggest that the mordenite crystals constituting the plate side have a crystalline structure different from that of the crystals formed on the hydrogel side, or that of the powder mordenite crystals.

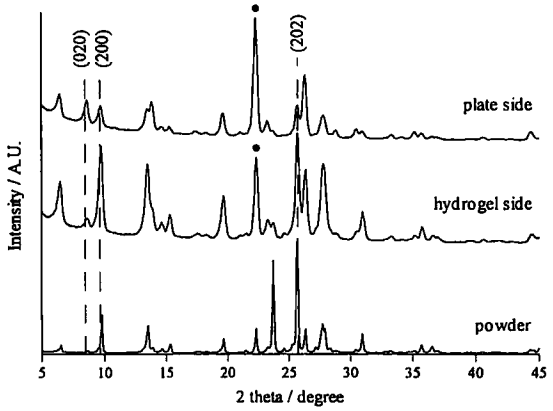

Figure 1. X-ray diffraction patterns of synthesized mordenite powder and membrane.

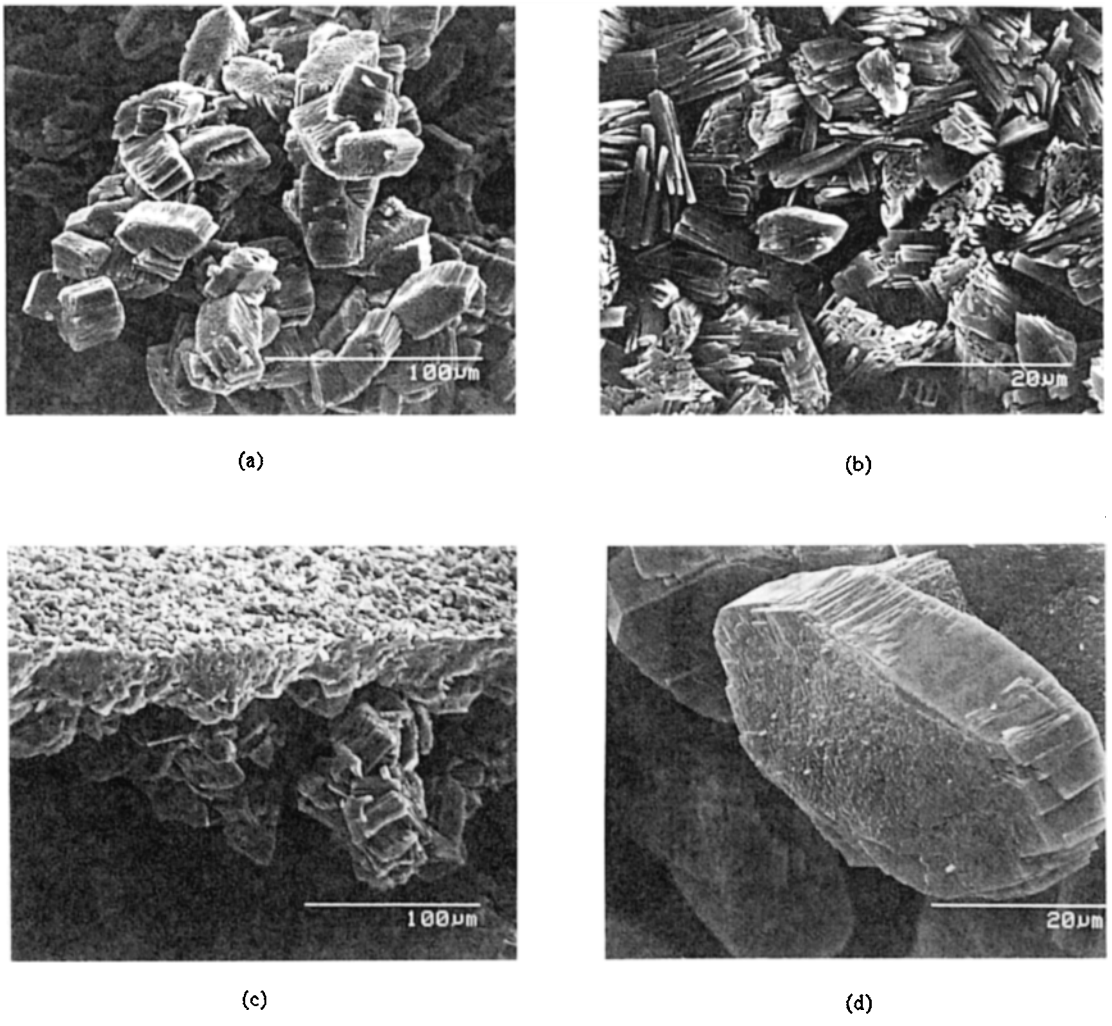

Figure 2. SEM photographs of synthesized mordenite powder and membrane; (a) Hydrogel side, (b) plate side, (c) cross section, and (d) powder.

Figure 2 shows SEM photographs of the synthesized mordenite membrane and powder; we find different crystal shapes on the hydrogel side (Fig. 2(a)) and plate side (Fig. 2(b)) of the mordenite membrane. The prismatic crystals formed on the hydrogel side of the synthesized membrane had the same crystal shape as that of the mordenite powder crystals (Fig. 2(d)). This evidence supports the above-described finding in X-ray diffraction analysis that the powder's diffraction pattern was the same as that of the hydrogel side. On the plate side, rectangular crystals in bundles collectively formed the membrane. A cross-sectional photograph (Fig. 2(c)) shows that the mordenite membrane is configured with two layers, i.e., a rectangular crystal layer and a prismatic crystal layer, the former accounting for about half the thickness of the mordenite membrane.

Nitrogen adsorption at 77 K was then measured on powder and on membrane. The adsorption isotherms obtained are shown in Fig. 3. The open circles are for the powder's adsorption isotherm, the closed circles for the membrane's. Table 1 shows the relative surface areas obtained by BET plot of the adsorption amount data, and the saturated adsorption amounts determined by Dubinin-Radushkevich (DR) plot. The EPMA-determined Si/Al ratios and framework compositions of powder and membrane are also shown in Table 1. The relative surface area and saturated

Table 1. Surface area, saturated adsorption amount (W_0), framework composition and Si/Al ratio.

	Surface area /$m^2 \cdot g_{dry}^{-1}$	W_0 /$cm^3 \cdot g_{dry}^{-1}$	Framework composition	Si/Al ratio
Powder	404	0.17	$Na_{6.6}Al_{6.6}Si_{41.4}O_{96}$	6.2
Membrane	211	0.09	$Na_{6.2}Al_{6.2}Si_{41.8}O_{96}$	7.0

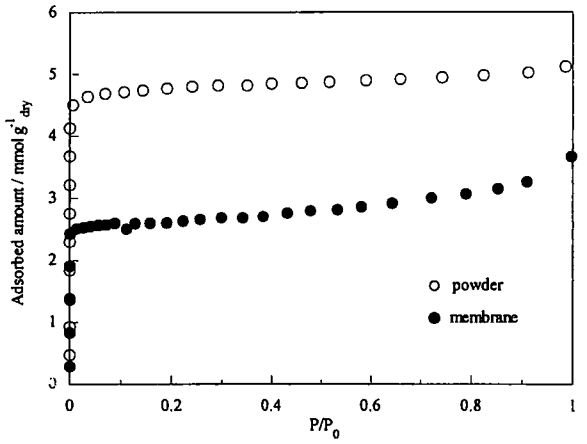

Figure 3. Adsorption isotherms of N_2 on synthesized mordenite powder and membrane.

adsorption amount of the powder were about 2 times those of the membrane. Since the powder's relative surface area agrees with the reference value presented by Japan Reference Catalysis (1993), formation of good mordenite crystals was confirmed. Concerning the framework compositions determined by EPMA, there was almost no difference between the powder and the membrane; it can therefore be assumed that they would have no differences in adsorption characteristic, or affinity for polar or nonpolar molecules. The membrane was expected to show the same adsorption amount as for the powder; actually, however, the amount of adsorption by the membrane was about half that by the powder. This finding suggests that the membrane's adsorption characteristic was affected by some other factors, since the powder had the same adsorption characteristic as that of ordinary mordenite crystals, as stated above.

Adsorption was then measured for various substances of different polarities and molecular cross-sectional areas. The results are shown in Fig. 4; Fig. 4(a) shows the powder's adsorption isotherms and Fig. 4(b) the membrane's. All the powder's adsorption isotherms were of the Langmuir type and all the

Table 2. Saturated adsorption amount (W_0) of powder and membrane determined from the adsorption of several adsorbents.

	W_0/$cm^3 \cdot g_{dry}^{-1}$ (U.C.$^{-1}$)				
	H_2O	N_2	Methanol	*n*-Hexane	*tert*-Butyl alcohol
Powder	0.14	0.17	0.19	0.06 (1.4)	0.02 (0.6)
Membrane	0.14	0.09	0.12	0.02	trace

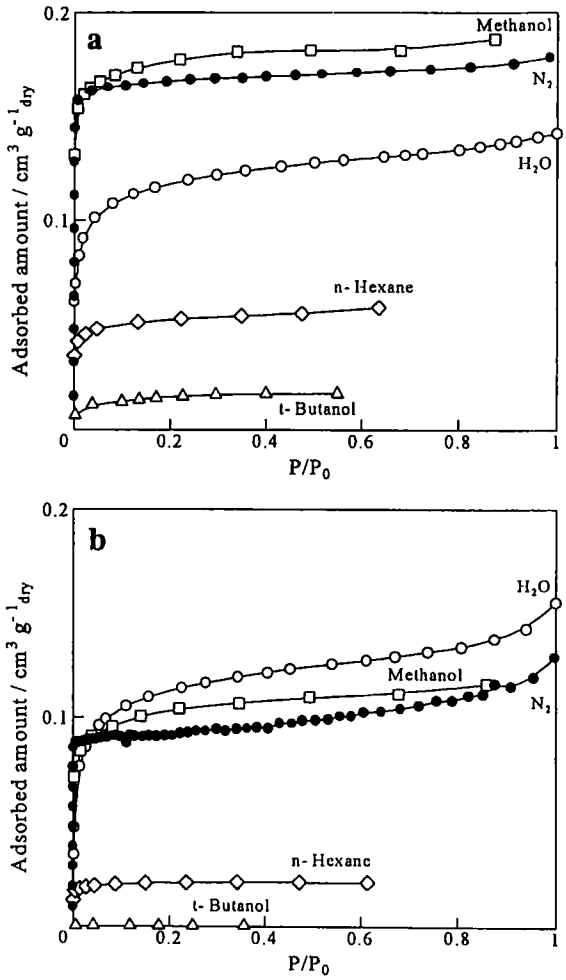

Figure 4. Adsorption isotherms of H_2O, methanol, *n*-hexane and *tert*-butyl alcohol on synthesized mordenite powder (a) and membrane (b).

membrane's adsorption isotherms were also of the Langmuir type except at higher equilibrium pressure. The saturated adsorption amounts for the respective adsorbates, determined from DR-plots, are shown in Table 2. The D-R plots were found to be linear except at initial stage of adsorption. In case of the membrane,

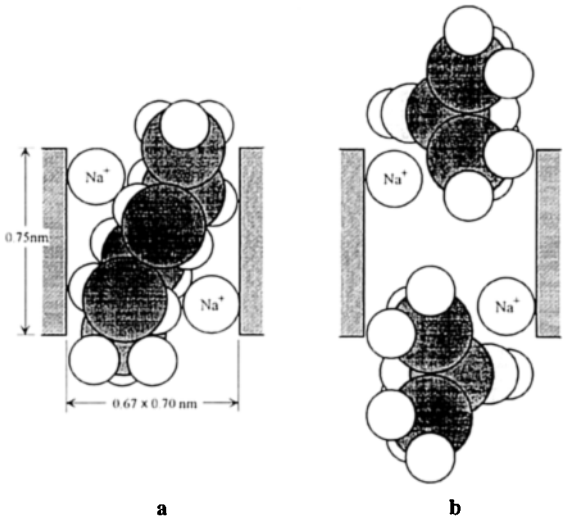

Figure 5. Adsorption state in the pore of mordenite of *n*-hexane (a) and *tert*-butyl alcohol (b).

however, a linear plot deviated at the highest equilibrium pressure for water and nitrogen, indicating the presence of mesopores. The adsorption amount was derived from a linear portion of DR-plots. For *n*-hexane (nonpolar) and *tert*-butyl alcohol (polar), which both have a large molecular cross-sectional area, the adsorption amount was considerably smaller than the amount of nitrogen adsorbed, irrespective of the presence or absence of molecular polarity. For methanol and water, both polar substances with small molecular cross-sectional area, the adsorption amount for both powder and membrane was nearly the same as that for nitrogen.

The adsorption states shown in Fig. 5 can be assumed for *n*-hexane and *tert*-butyl alcohol. Considered with the Si/Al ratio of mordenites synthesized in the present study, about 2 cations are present per main channel (Itabashi et al., 1989). Since *n*-hexane, though a linear molecule, has a freely bendable molecular chain, the adsorption state of Fig. 5(a) is suggested. If such adsorption occurs, we can assume that mordenite, capable of adsorbing about 0.7 molecules of *n*-hexane per main channel, will adsorb no more than 1.4 molecules (0.7×2) into its pores, because it has two main channels per unit cell. As shown in Table 2, the powder's saturated adsorption amount for *n*-hexane was 1.4 molecules per unit cell, the maximum possible adsorption of *n*-hexane afforded by the stereo configuration of its molecule. As for *tert*-butyl alcohol, a polar substance having a greater molecule size, strong interaction with the cations in the main channels is expected. It is likely that this interaction prevented the entrance of more *tert*-butyl alcohol molecules into the main channels, as shown in Fig. 5(b), resulting in the very low adsorption amount. In the case of water, membrane and powder had the same saturated adsorption amount, in contrast to the other adsorbable substances tested, in which the membrane's saturated adsorption amount was about half that of the powder. This suggests the presence of deformed pores in the membrane that are capable of selectively adsorbing the water molecule.

In a previous study by X-ray diffraction analysis and SEM observation, we clarified the mechanism of mordenite membrane formation shown in Fig. 6 (Yamazaki and Tsutsumi, 1995). The framework of mordenite is known to consist of secondary·building units (SBUs), as shown in the upper right of Fig. 6 (Breck, 1974). Such SBUs, as dimers, align along the 001 axis and set in parallel with each other to form the (110) face. From the thus-formed (110) faces are formed rectangular crystals, as SBU dimers oriented along the 001 axis are stacked along the $\bar{1}10$ or $1\bar{1}0$ axis. These rectangular crystals are formed on PTFE substrate, resulting in the formation of a rectangular crystal membrane. It is assumed that crystal growth does not proceed to the formation of hexagonal prismatic crystals because the motional freedom of crystallites is affected due to crystallization on the substrate, hampering crystal growth along the *a*- or *b*-axis. Another possible reason is that mutually adjacent crystallites failed to grow into complete crystal form due to mutual inhibition of their growth. As is evident from SEM observations, the prismatic crystal layer, which forms the second layer of the membrane, should result from the linkage of mordenite crystals present in the hydrogel to the rectangular crystal layer via SBUs. Since the prismatic crystal layer of the double-layered mordenite membrane has the same crystalline structure as that of the powder, they are assumed to show the same adsorption behavior. In other words, deformed pores, if present, occur in the rectangular crystal layer, which is formed in the initial stage of membrane synthesis.

Figure 7 shows a mechanism assumed to be involved in the deformed pore formation. Ideally, the membrane has a pore structure in which pores align continuously in parallel with the membrane's horizontal plane. Actually, however, crystallite shift occurs, as shown in Fig. 7; the resulting gaps are assumed to constitute such deformed pores. This mechanism can

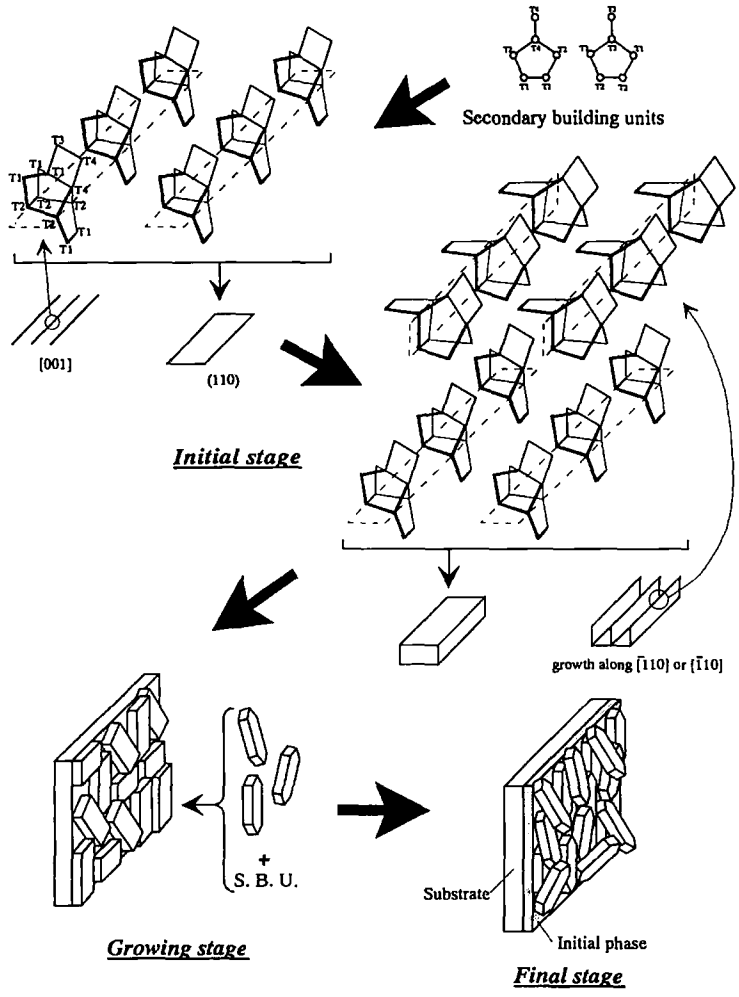

Figure 6. Formation mechanism of mordenite membrane on substrate.

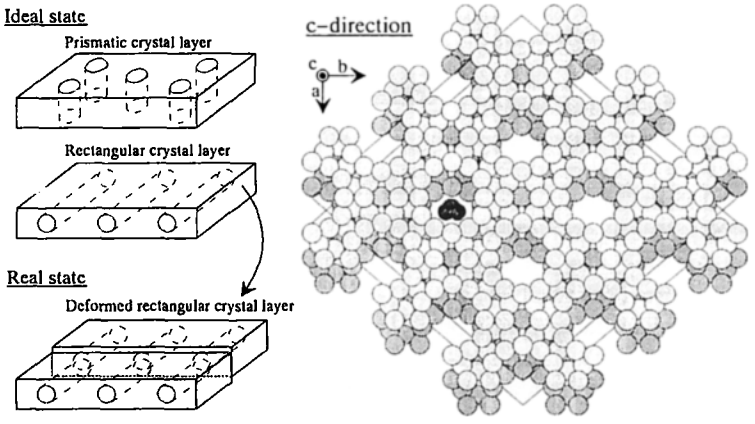

Figure 7. Model of deformed pore structure of synthesized mordenite membrane.

be explained with reference to the *c*-axis projection of Fig. 7, including framework oxygen atoms, as follows: upon crystallite shifts as indicated by the light and dark shades, pores allowing the entrance of water molecules are formed. These pores serve as barriers (pore walls) against molecules larger than the water molecule to prevent their entrance, resulting in deformed pores. Such crystallite shifts are also suggested by the results of X-ray diffraction analysis. The intensity of the (002) diffraction peak near 24 degrees in Fig. 1 decreased in the membrane, in comparison with the powder. On the plate side of the membrane, in particular, the (002) peak decreased considerably. This decrease in the diffraction intensity of (002) suggests that the periodic continuous structure along the *c*-axis has been destroyed more in the membrane than in the powder. SEM observation confirmed that the rectangular crystals on the plate side grew best along the *c*-axis. It appears, however, that the crystallite shifts are not parallel with each other on the *ab* plane, but involve slight distortion, since the diffraction intensity of (002) was decreased.

Studies on the mordenite membrane synthesis in short crystallization are now in progress in order to confirm the formation of the deformed pore in the initial stage of membrane formation. Furthermore, effects of the cation in main channel on the adsorption amount will be reported in the future.

Conclusion

The mordenite membrane formed on PTFE substrate was found to be configured with two layers of different crystal forms: initially formed rectangular crystal layer, and subsequently formed prismatic crystal layer. The adsorption behavior of this membrane differed from that of the powder. For adsorbable substances other than water, only the prismatic crystal layer, having the same crystal form as that of the powder, is involved in adsorption. The rectangular crystal layer, formed in the initial stage of membrane synthesis, was found to contain deformed pores capable of exclusively adsorbing water molecules. It can be concluded that these deformed pores result from shifts of crystallites on the *ab* plane in the rectangular crystal layer, and that these shifts are not perpendicular to the *c*-axis but involve slight distortion.

References

Barrer, R.M., "Synthesis and Reactions of Mordenite," *J. Chem. Soc.*, 2158–2163 (1948).

Boom, J.P. et al., "Zeolite Filled Membrane for Gas Separation and Pervaparation," *Stud. Surf. Sci. Cat.*, **84**, 1167–1174 (1994).

Breck, D.W. (Ed.), *Zeolite Molecular Sieves*, p. 122, John Wiley & Sons, New York, 1974.

Itabashi, K., T. Okabe, and K. Igawa, *Proc. of the 7th International Zeolite Conf.*, Y. Murakami, A. Iijima, and J.W. Ward (Eds.), pp. 369–376, Kodansha, Tokyo, 1989.

Kranich, W.L. et al., "Properties of Aluminum-Deficient Large-Port Mordenites," *Advan. Chem. Ser.*, **101**, 502–512 (1971).

Manual of Reference Catalysis, Catalyst Society of Japan (1993).

Sano, T. et al., "Steaming of ZSM-5 Zeolite Film," *Zeolites*, **12**, 131–134 (1992).

Sano, T. et al., "Potentials of Silica Membranes for the Separation of Alcohol/Water Mixture," *Stud. Surf. Sci. Cat.*, **84**, 1175–1182 (1994).

te Hennepe, H.J.C. et al., "Zeolite-Filled Silicon Rubber Membranes Part 1. Membrane Preparation and Pervaparation Results," *J. Mem. Sci.*, **35**, 39–55 (1987).

Tsikoyiannis, J.G. and W.O. Haag, "Synthesis and Characterization of a Pure Zeolite Membrane," *Zeolites*, **12**, 126–130 (1992).

Ueda, S., H. Murata, and M. Koizumi, "Crystallization of Mordenite from Aqueous Solution," *Am. Mineral.*, **65**, 1012–1019 (1980).

von Ballmoos, R. and J.B. Higgins, "Collection of Simulated XRD Powder Patterns for Zeolites," *Zeolites*, **10**, 448–449 (1990).

Yamazaki, S. and K. Tsutsumi, "Synthesis of an A-Type Zeolite Membrane on Silicon Oxide Film-Silicon, Quartz Plate and Quartz Fiber Filter," *Microporous Mater.*, **4**, 205–212 (1995).

Yamazaki, S. and K. Tsutsumi, "Synthesis of a Mordenite Membrane on a Stainless-Steel Filter and Polytetrafluoroethylene Plate Substrates," *Microporous Mater.*, **5**, 245–253 (1995).